IMU-Based Motion Estimation for Assistive Exoskeleton Control in High-Load Tasks and Complex Environments

Aderajew Tilahun [1], Jeronimo Cox[1], Tomonari Furukawa [1],Gamini Dissanayake [2]

Abstract— **This paper presents a real-time spatial motion estimation framework based on Inertial Measurement Unit (IMU) sensors that fuses gyroscope, accelerometer, and dual opposite-sided magnetometer data via an Extended Kalman Filter (EKF) with integrated online calibration. The core contribution is a novel magnetometer calibration technique that combines the ambient noise suppression capability of dual magnetometers with real-time estimation of hard and soft iron distortion parameters. These calibration parameters are incorporated in the EKF state and are continuously updated, allowing for adaptive compensation for hard and soft iron distortion. The proposed method achieves robust, drift-corrected orientation estimation in magnetically disturbed, GPS-denied, and vision-free environments - conditions common in construction sites. The proposed approach was experimentally validated on a human arm, demonstrated superior accuracy compared to the conventional approaches. The ability to estimate accurate and drift free motion online using wearable IMU sensors makes this framework well-suited for wearable robotics and assistive exoskeleton control in complex field environments.**

I. Introduction

Human–Robot Interaction (HRI) plays a vital role in assistive technologies that aim to prevent injuries and help workers undertaking physically demanding tasks, such as moving heavy items. Exoskeletons offer a viable approach to alleviate musculoskeletal strain and improve physical performance [1]. Real-time orientation tracking is essential for maintaining ergonomic posture and achieving seamless HRI [2]. Various motion tracking methods have been proposed. While optical motion tracking systems offer high accuracy but requires clear line-of-sight, making it unsuitable for cluttered environments. Electromyography detects muscle activation well but suffers from signal fluctuation and placement sensitivity [3]. Recently, inertial motion tracking has gained interest, particularly in scenarios where significant occlusions obstructing vision exist, due to their independence from external infrastructure and the use of miniature inertial measurement units (IMUs) [4]. However, drift due to integration is inherent when an IMU is used for ego-motion estimation. To mitigate this, additional sensors such as GPS [5], ultrawideband (UWB) [6], visual devices [7], and magnetometers [8] [9] are often employed to correct this drift. However, these sensors face limitations: GPS is unreliable in indoor, UWB suffers in occluded settings, and magnetometers are prone to magnetic interference. As a result, minimizing IMU drift remains a key challenge in inertial motion tracking system.

Existing methods for improving inertial motion tracking fall into three main categories: hardware enhancements, sensor modeling and calibration, sensor fusion. Traditional sensor hardware settings have seen accelerometers for pitch and roll, gyroscopes for angular velocity, and magnetometers for heading [10]. Accelerometers can reliably estimate tilt under quasi-static situations due to their capacity to monitor gravity. However, their accuracy is limited by sensor bias and noise. Magnetometers provide absolute heading but are highly susceptible to magnetic disturbances [11], particularly in places like construction sites where strong and non-uniform magnetic interference is prevalent. To address these sensor-specific limitations, numerous modeling and calibration techniques have been developed. Among them, magnetometer calibration has received significant attention because of its vital role in drift-free orientation correction, and it is often classified into into offline and online approaches.

Offline techniques, such as ellipsoid fitting and its 3D extensions [12], aim to correct hard and soft iron distortions. While effective in static and uniform magnetic fields, these methods rely on pre-collected calibration data and perform poorly in dynamic or changing environments. In contrast, online calibration techniques adapt in real time and are better suited for non-uniform magnetic conditions by continuously tuning calibration parameters to mitigate current distortions. Several studies have explored online calibration using filtering and modeling approaches [13], [14]. Although these methods provide adaptive correction, they often fail to explicitly address ambient magnetic interference, which can vary rapidly in cluttered or electromagnetically active environments. To address this, recent work [9] proposed an online calibration method using oppositely facing coupled magnetometers to estimate and reject shared environmental magnetic noise in real time. While effective against ambient interference, this approach does not correct for soft iron distortions, which deform the magnetic field shape and degrade orientation accuracy.

These problems highlight the necessity for a real-time framework capable of handling both ambient and local distortions while also facilitating multi-sensor fusion. The Extended Kalman Filter (EKF) is a frequently used Kalman filter type for this purpose [10], [15], allowing for fast recursive Bayesian estimation (RBE) under Gaussian uncertainty assumptions. This paper presents a novel magnetometer calibration method that combines dual opposite-sided magnetometers with an EKF-based online calibration

[1]VICTOR Lab, University of Virginia, Charlottesville VA, 22904, USA {mub4pn,wrr9nb,tomonari}@virginia.edu

[2]Mechanical and Mechatronic Engineering, University of Technology, Sydney gamini.dissanayake@uts.edu.au

framework to address magnetic distortion in non-uniform complex environments. The magnetometer calibration parameters, bias and scale are embedded in the EKF state and updated online for adaptive correction of hard and soft iron distortion. Then, by fusing gyroscope input for short-term stability with calibrated magnetometer and accelerometer data for long-term correction, the proposed method enables accurate orientation estimation in magnetically disturbed, GPS-denied, and vision-free environments.

II. Mathematical Model of the Proposed System

2.1 Human Body Kinematic Model

The full human body is modeled as a kinematic chain of n rigid links, each connected by joints. Each link $i \in \{1, 2, \ldots, n\}$ is with an sensor suite containing a gyroscope, accelerometer, and a dual magnetometers. The orientation of each link $\mathbf{q}_i$ is estimated independently via EKF, and full-body pose is reconstructed using the known anatomical geometry.

2.2 Sensor Models

Each IMU provides the following measurements:

2.1.1. Gyroscope

$$\boldsymbol{\omega}_i^m = \boldsymbol{\omega}_i + \mathbf{b}_{g,i} + \mathbf{v}_{g,i} \tag{1}$$

where $\boldsymbol{\omega}_i^m$ is the measured angular velocity, $\boldsymbol{\omega}_i$ is the true angular velocity, $\mathbf{b}_{g,i}$ is the gyroscope bias, and $\mathbf{v}_{g,i} \in \mathbb{R}^3$ is zero-mean Gaussian sensor noise.

2.1.2. Accelerometer

$$\mathbf{a}_i^m = \mathbf{R}(\mathbf{q}_i)^\top \cdot \mathbf{g} + \mathbf{v}_{a,i} \tag{2}$$

where $\mathbf{a}_i^m$ measured acceleration in the body frame, $\mathbf{g} = [0, 0, -g]^\top$ is the gravity vector in the global frame, and $\mathbf{v}_{a,i} \in \mathbb{R}^3$ is accelerometer measurement noise.

2.1.3 Magnetometer (Dual Opposite-Sided)

$$\mathbf{B}_i^{\text{diff}} = \frac{1}{2}\left(\mathbf{B}_i^{(1)} - \mathbf{B}_i^{(2)}\right) \tag{3}$$

where $\mathbf{B}_i^{(1)}$ and $\mathbf{B}_i^{(2)}$ raw measurement from sensor 1 and sensor 2, respectively.

$$\mathbf{B}_i^{\text{cal}} = \mathbf{S}_i^{-1}\left(\mathbf{B}_i^{\text{diff}} - \mathbf{b}_{m,i}\right) \tag{4}$$

where $\mathbf{B}_i^{\text{cal}}$ is the calibrated magnetometer reading in the body frame from dual magnetometers, $\mathbf{S}_i = \text{diag}(s_x, s_y, s_z)$ is the soft iron scale matrix, and $\mathbf{b}_{m,i} \in \mathbb{R}^3$ is the hard iron bias vector.

III. EKF-Based Sensor Fusion and Online Calibration

In this framework, gyroscope, accelerometer, and calibrated magnetometer data are fused within the EKF, as shown in Figure 1. Each links orientation and magnetometer calibration parameters are estimated using an EKF.

3.1 State Vector: The EKF estimates the following state vector for each link i at time k:

$$\mathbf{x}_{i,k} = \begin{bmatrix} \mathbf{q}_{i,k} \\ \mathbf{b}_{m,i,k} \\ \mathbf{s}_{m,i,k} \end{bmatrix} \in \mathbb{R}^{10} \tag{5}$$

where $\mathbf{q}_{i,k}$ is the orientation quaternion, $\mathbf{b}_{m,i,k}$ is the magnetometer bias, and $\mathbf{s}_{m,i,k}$ is the scale vector.

3.2 Prediction Step: Orientation is propagated using gyroscope measurements:

$$\mathbf{q}_{i,k} = \mathbf{q}_{i,k-1} \otimes \text{Quat}\left(\frac{1}{2}(\boldsymbol{\omega}_{i,k}^m - \mathbf{b}_{g,i,k})\Delta t\right) \tag{6}$$

where $\otimes$ denotes quaternion multiplication and $\text{Quat}(\cdot)$ converts angular velocity into a quaternion increment.

3.3 Correction Step: In an EKF, the sensor measurement is typically expressed as a nonlinear observation model.

3.3.1 Accelerometer Measurement Model in EKF

The accelerometer is modeled as:

$$\mathbf{z}_{i,k}^a = \mathbf{h}_a(\mathbf{x}_{i,k}) + \mathbf{v}_{a,i,k} \tag{7}$$

Where $\mathbf{z}_{i,k}^a = \mathbf{a}_{i,k}^m$, $\mathbf{h}_a(\mathbf{x}_{i,k}) = \mathbf{R}(\mathbf{q}_{i,k})^\top \cdot \mathbf{g}$

3.3.2 Magnetometer Measurement Model in EKF

For the magnetometer, the EKF compsres the calibrated sensor reading to the expected magnetic field in the body frame.The expected magnetic field, based on the estimated orientation $\mathbf{q}_i$, is given by:

$$\mathbf{h}_m(\mathbf{x}_{i,k}) = \mathbf{R}(\mathbf{q}_{i,k})^\top \cdot \mathbf{B}_{\text{ref}} \tag{8}$$

The EKF measurement equation becomes:

$$\mathbf{z}_{i,k}^m = \mathbf{B}_{i,k}^{\text{cal}} = \mathbf{R}(\mathbf{q}_{i,k})^\top \cdot \mathbf{B}_{\text{ref}} + \mathbf{v}_{m,i,k} \tag{9}$$

where $\mathbf{R}(\mathbf{q}_{i,k})$ is the rotation matrix corresponding to the orientation quaternion $\mathbf{q}_{i,k}$, $\mathbf{B}_{\text{ref}}$ is the known Earth magnetic field vector in the global frame, $\mathbf{v}_{m,i,k} \in \mathbb{R}^{3n}$ is Gaussian magnetometer noise.

Since the magnetometer sensors only provide raw readings, thus the calibrated measurement $\mathbf{B}_{i,k}^{\text{cal}}$ is computed internally using the current EKF estimates state (bias and scale). This allows the EKF to dynamically compensate magnetic distortions. The technique allows for continuous and robust orientation estimation by correcting gyroscope drift using calibrated magnetic measurements.

IV. Experiment and Results

4.1 Experiment Setup

To evaluate and validate the proposed method, human arm motion experiments were conducted using a wearable IMU sensor suit with OptiTrack markers, as shown in Figure 2. Each sensor module included a dual-magnetometer setup (LIS3MDL) and an IMU (BNO055) with a gyroscope and accelerometer. Joint orientation estimates from two arm segments were compared against ground truth from an OptiTrack motion capture system.

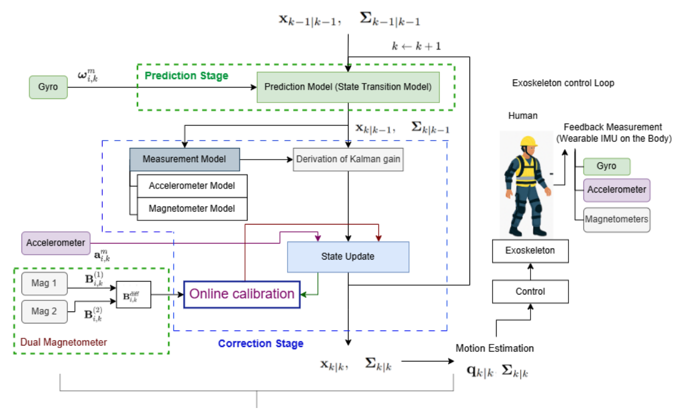

Fig. 1. EKF-Based Sensor Fusion and Online Magnetometer Calibration

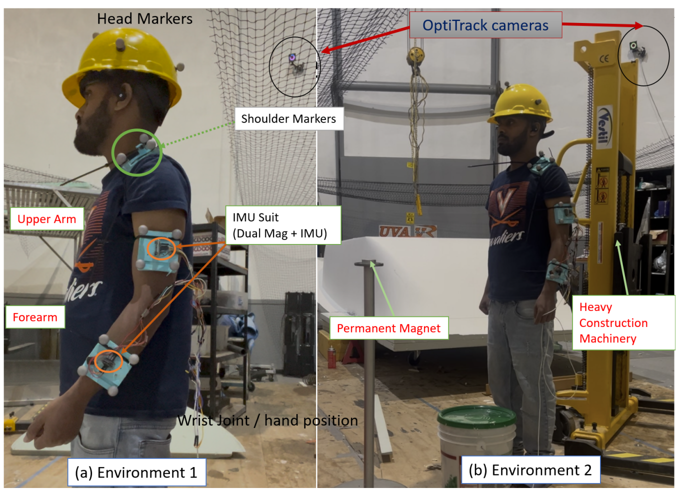

Fig. 2. Experimental Setup

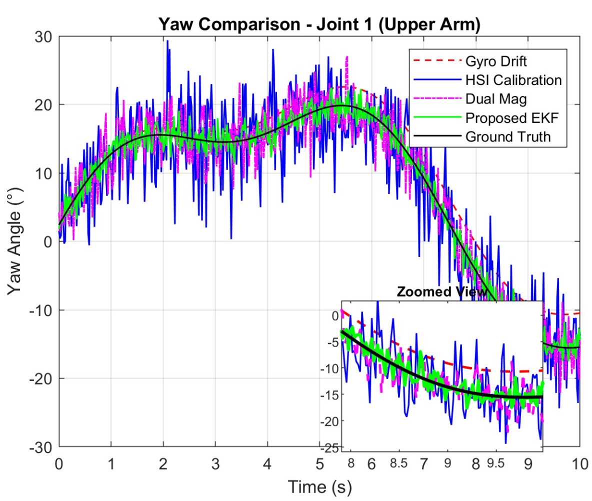

Fig. 3. Joint 1 Yaw Angle Comparison with Ground Truth

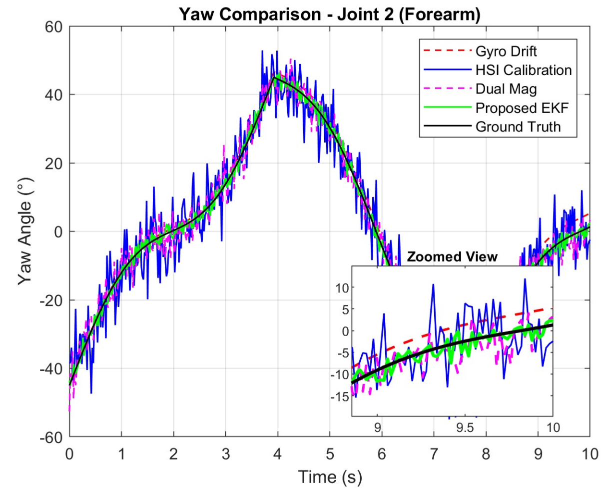

Fig. 4. Joint 2 Yaw Angle Comparison with Ground Truth

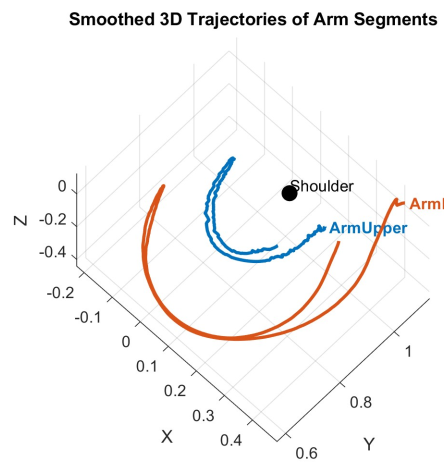

Fig. 5. 3D Motion Trajectory of Arm Links – Ground Truth

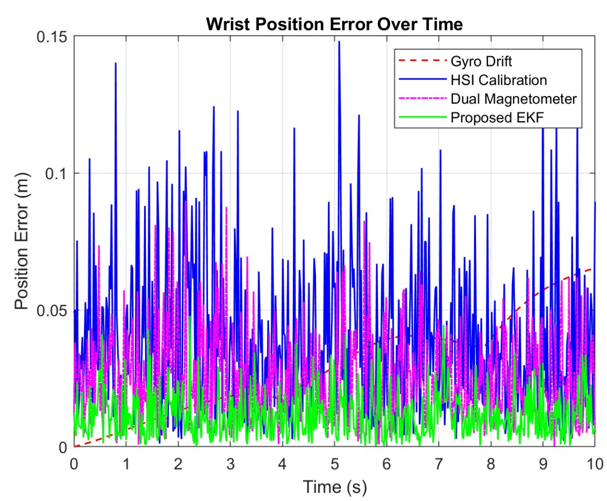

Fig. 6. Wrist Position Trajectory error Comparison (3D Euclidean distance)

4.2 Result and Analysis

To evaluate the accuracy under magnetically distorted conditions, three calibration methods were tested using the same IMU sensor suite: offline ellipsoid fitting (HSI) calibration, dual opposite-sided magnetometers without updating the hard and soft iron calibration parameters, and the proposed method. All methods were implemented within the same EKF sensor fusion framework to ensure a fair comparison. Magnetic disturbances were introduced by placing a permanent magnet and ferrous objects near the system, as shown in Figure 2(b), representing Environment 2. Offline calibration was first performed in a relatively undisturbed setting, referred to as Environment 1 (Figure 2(a)).

TABLE I
YAW ANGLE ESTIMATION ERROR COMPARISON

Metric	Joint 1			Joint 2		
	HSI	**Dual**	**Proposed**	**HSI**	**Dual**	**Proposed**
RMSE (°)	5.248	3.217	1.391	7.247	4.259	2.818
MAE (°)	4.214	3.180	1.103	5.902	3.238	2.131

As shown in Figures 3 and 4, the proposed method consistently tracked the ground truth yaw angles for both joints with minimal error, even with magnetic interference and soft iron distortion. The HSI calibration experienced significant inaccuracies when the magnetic environment changed. The dual magnetometer approach, while effective against ambient noise, did not address soft iron distortions. The results in Table 1 confirm the superiority of the proposed method yields the lowest estimation errors, with RMSE of 1.391° and 2.818°, and MAE of 1.103° and 2.131° for Joint 1 and Joint 2, respectively.

TABLE II
POSITION TRAJECTORY ERROR COMPARISON METRICS

	MAE (m)	**RMSE (m)**	**Max Error (m)**
HSI Calibration	0.0461	0.0560	0.1404
Dual Magnetometer	0.0251	0.0316	0.1080
Proposed	**0.0118**	**0.0148**	**0.0443**

To evaluate full pose estimation, forward kinematics was applied to compute the 3D wrist position using the estimated joint orientations and known anatomical link lengths, with the shoulder defined as the anchor point. Ground truth global position data was obtained from the OptiTrack system. As shown in Figure 5, the position trajectories of each limb segment were recorded and used to reconstruct the wrist trajectory based on the estimated orientation and shoulder position. The resulting wrist trajectories were then compared across different calibration and estimation methods. Figure 6 illustrates the corresponding position errors. As summarized in Table 2 the proposed method consistently outperformed the others under magnetically distorted conditions.

V. CONCLUSIONS

This paper introduced an EKF-based sensor fusion framework that incorporates gyroscope, accelerometer, and dual opposite-sided magnetometers with online magnetometer calibration. By embedding hard and soft iron calibration parameters into the EKF state and updating them in real time, the system adaptively compensates for both ambient and device-local magnetic distortions. Experimental validation on a human arm motion tracking setup demonstrated superior orientation accuracy over conventional methods. These results highlight its potential for reliable motion tracking in magnetically complex environments, supporting real-time control in wearable robotics and assistive exoskeletons.

ACKNOWLEDGEMENT

This work was primarily supported by the Office of Naval Research, Grant N00014-23-1-2572. The authors would like to express their gratitude to Dr. Thomas McKenna, who is the program manager of the project. Partial support by Honda Motor is also acknowledged.

REFERENCES

[1] Cai, Min, et al. "Safety evaluation of human–robot collaboration for industrial exoskeleton." Safety science 164 (2023): 106142.
[2] Kim, Wansoo, et al. "A human-robot collaboration framework for improving ergonomics during dexterous operation of power tools." Robotics and Computer-Integrated Manufacturing 68 (2021): 102084.
[3] Nazari, Farhad, et al. "Applied exoskeleton technology: A comprehensive review of physical and cognitive human–robot interaction." IEEE Transactions on Cognitive and Developmental Systems 15.3 (2023): 1102-1122.
[4] Tanenhaus, M., et al. "Miniature IMU/INS with optimally fused low drift MEMS gyro and accelerometers for applications in GPS-denied environments." Proceedings of the 2012 IEEE/ION Position, Location and Navigation Symposium. IEEE, 2012.
[5] Raveena, Ch S., et al. "Sensor fusion module using IMU and GPS sensors for autonomous car." 2020 IEEE International Conference for Innovation in Technology (INOCON). IEEE, 2020.
[6] Shi, Yutong, et al. "IMU/UWB fusion method using a complementary filter and a Kalman filter for hybrid upper limb motion estimation." Sensors 23.15 (2023): 6700.
[7] Shin, Soyong, Zhixiong Li, and Eni Halilaj. "Markerless motion tracking with noisy video and imu data." IEEE Transactions on Biomedical Engineering 70.11 (2023): 3082-3092.
[8] Zhang, Wei, J. Josiah Steckenrider, and Tomonari Furukawa. "Motion Tracking of a High-Speed Multilink System Using Dynamic Measurements Fusion." Journal of Dynamic Systems, Measurement, and Control 146.2 (2024).
[9] J. Cox, W. Zhang and T. Furukawa, "Motion Tracking with Coupled Magnetometers and Dynamic IMU Measurement Fusion in Nonuniform Magnetic Fields," 2023 26th International Conference on Information Fusion (FUSION), Charleston, SC, USA, 2023, pp. 1-8, doi: 10.23919/FUSION52260.2023.10224146.
[10] Xing, Yunlong, et al. "Design and Implementation of Motion Tracking System Based on IMU." 2024 IEEE 13th Data Driven Control and Learning Systems Conference (DDCLS). IEEE, 2024.
[11] Truppa, L., et al. "Magnetic-free quaternion-based robust unscented Kalman filter for upper limb kinematic analysis." IEEE Sensors Journal 23.3 (2022): 3212-3219.
[12] Fan, Beibei, et al. "Error Compensation of Three-axis Magnetic Sensor Based on Improved Ellipsoidal Fitting Method." IEEE Transactions on Magnetics (2025).
[13] J. Wang, Z. Deng, K. Shen, and Y. Bo, "Recurrent EKF-Based Inertial Aided Magnetometer Online Calibration for Complex Interference Environment," IEEE Transactions on Industrial Electronics, vol. 72, no. 1, pp. 1043–1055, 2025.
[14] Wu, Yuanxin, et al. "Dynamic magnetometer calibration and alignment to inertial sensors by Kalman filtering." IEEE Transactions on Control Systems Technology 26.2 (2017): 716-723.
[15] Simanek, Jakub, Michal Reinstein, and Vladimir Kubelka. "Evaluation of the EKF-based estimation architectures for data fusion in mobile robots." IEEE/ASME transactions on mechatronics 20.2 (2014): 985-990.